

Electronic Supporting Information

Enhanced Optical, Electrical and Mechanical Properties in Fluorine-Doped Tin Oxide Transparent Electrodes

Jaewon Kim^a, Sherman Wong^a, Gahui Kim^b, Young-Bae Park^b, Joel van Embden^a, Enrico Della Gaspera^{a,}*

^a School of Science, RMIT University, Melbourne VIC 3000, Australia

^b School of Materials Science and Engineering, Andong National University, Andong 36729, Korea.

Corresponding author: *enrico.dellagaspera@rmit.edu.au

Figure S1. XRD patterns with normalized intensity for FTO20 thin films deposited at various temperatures (same data as Figure 2a).

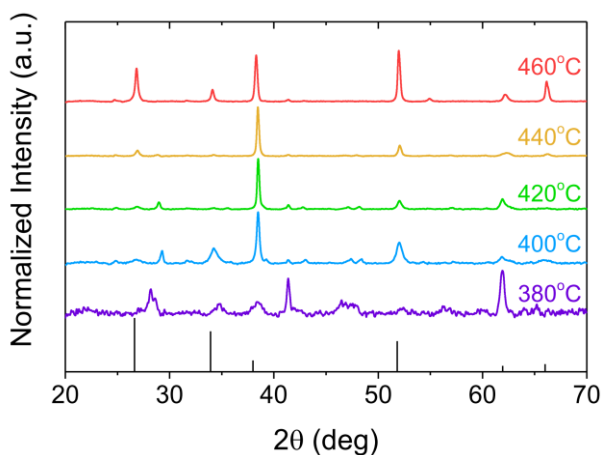


Figure S2. a) XRD patterns and b) crystallite size for FTO thin films deposited at 440 °C with different fluorine concentration.

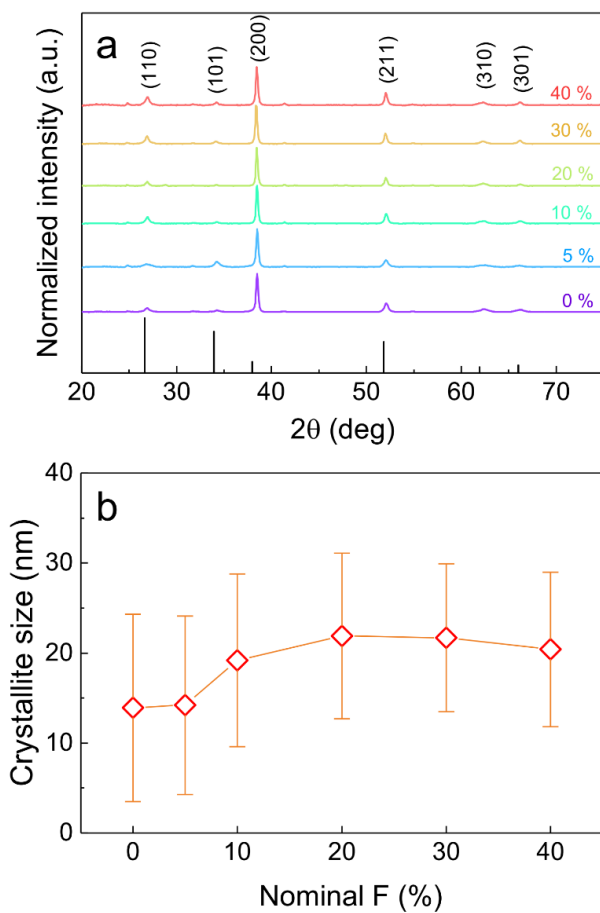


Figure S3. Texture coefficient for films deposited at 440 °C with varying fluorine nominal concentration.

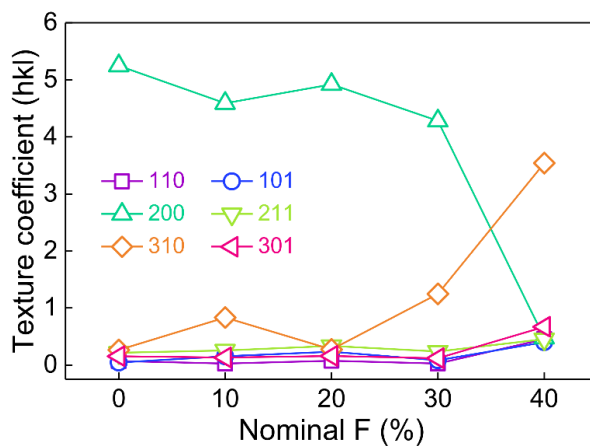


Figure S4. Cross-sectional SEM micrographs for FTO samples deposited at different pyrolysis temperatures. The scale bar is 400 nm and is common to all panels.

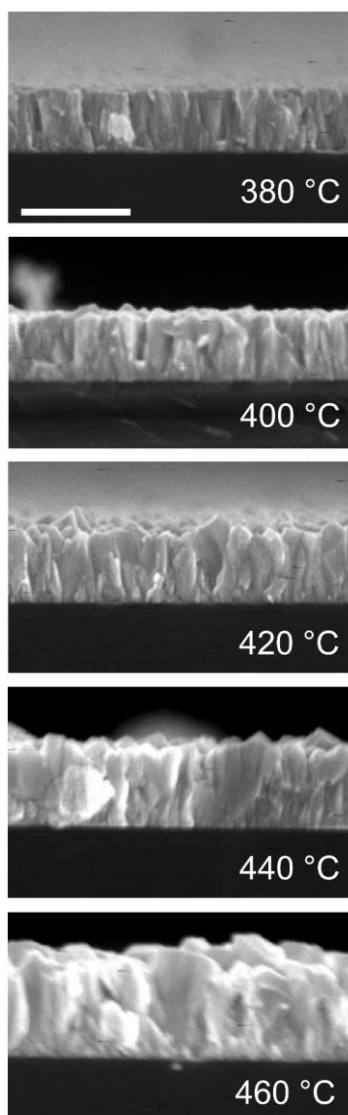


Figure S5. SEM micrographs for the FTO20 film deposited at 440 °C with different F concentration, from 0% (undoped) to 40%. The scale bar is 500 nm and is common to all panels. The bottom panel is a plot of grain density as a function of fluorine concentration.

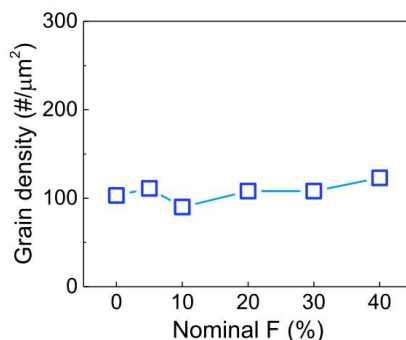
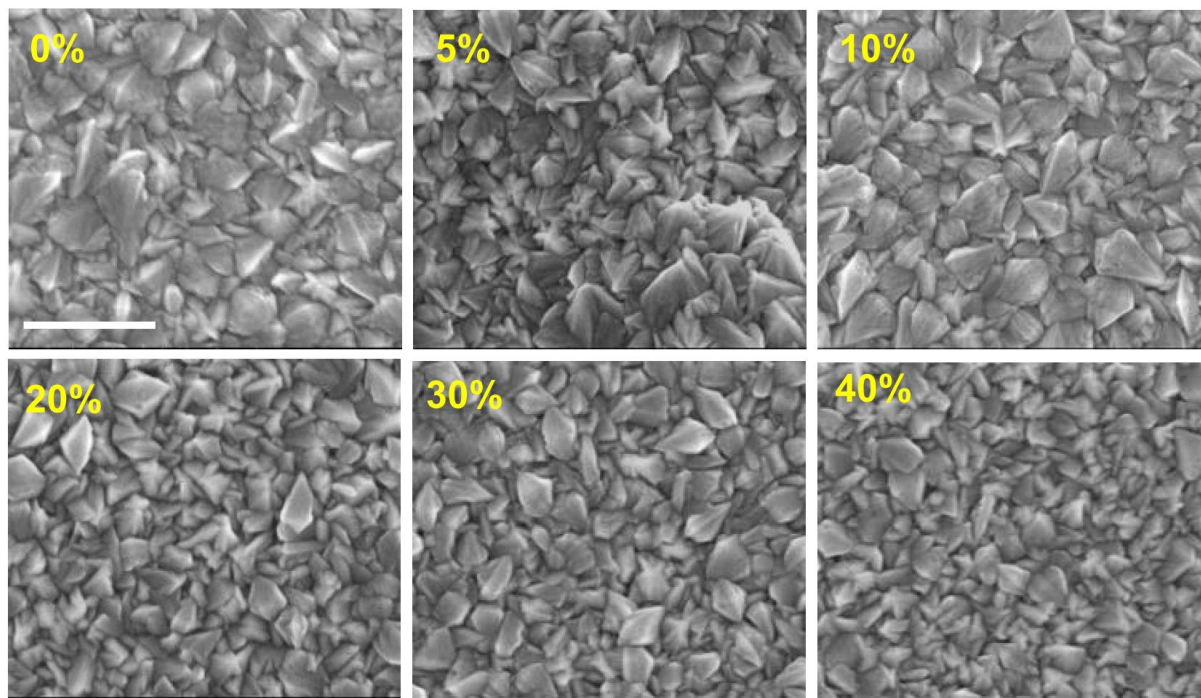


Figure S6. Carrier concentration, mobility and resistivity for FTO films deposited at 440 °C with varying fluorine concentration.

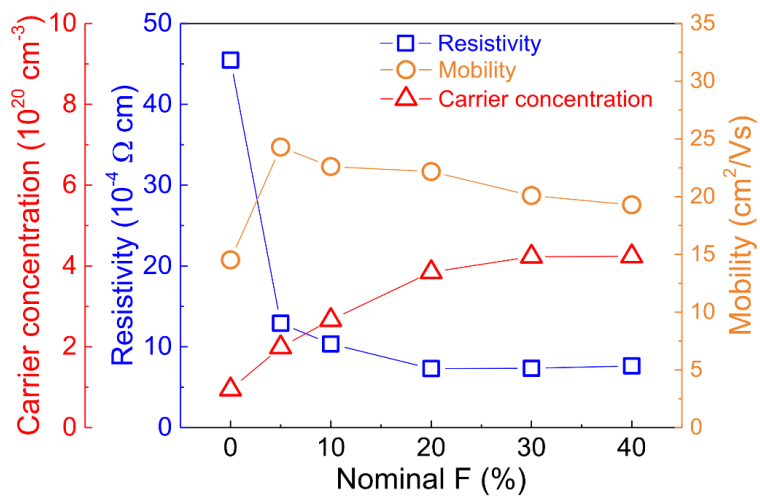


Figure S7. Sheet resistance of a typical FT020 sample measured at different temperatures.

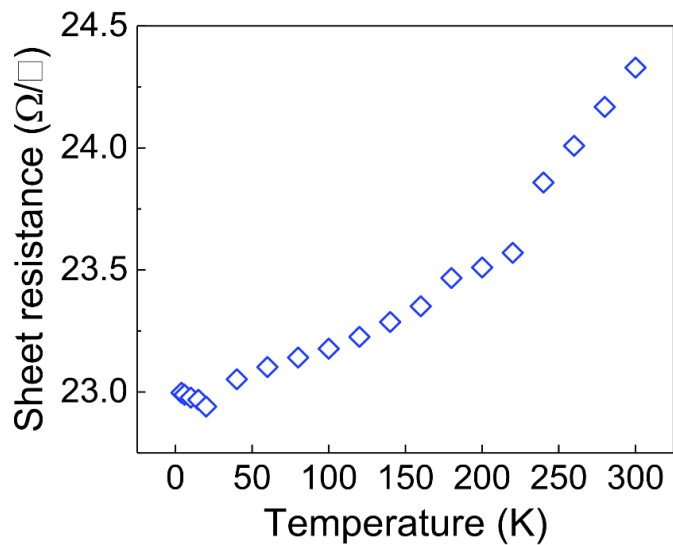


Figure S8. Optical characterization of FTO thin films deposited at 440 °C as a function of fluorine concentration. a) Transmittance spectra. b) Absorbance spectra normalized according to the sample thickness to take into account variation in intensity of the infrared signal due to the amount of material probed. c) Carrier concentration and normalized absorbance at 2500 nm as a function of the amount of fluorine doping.

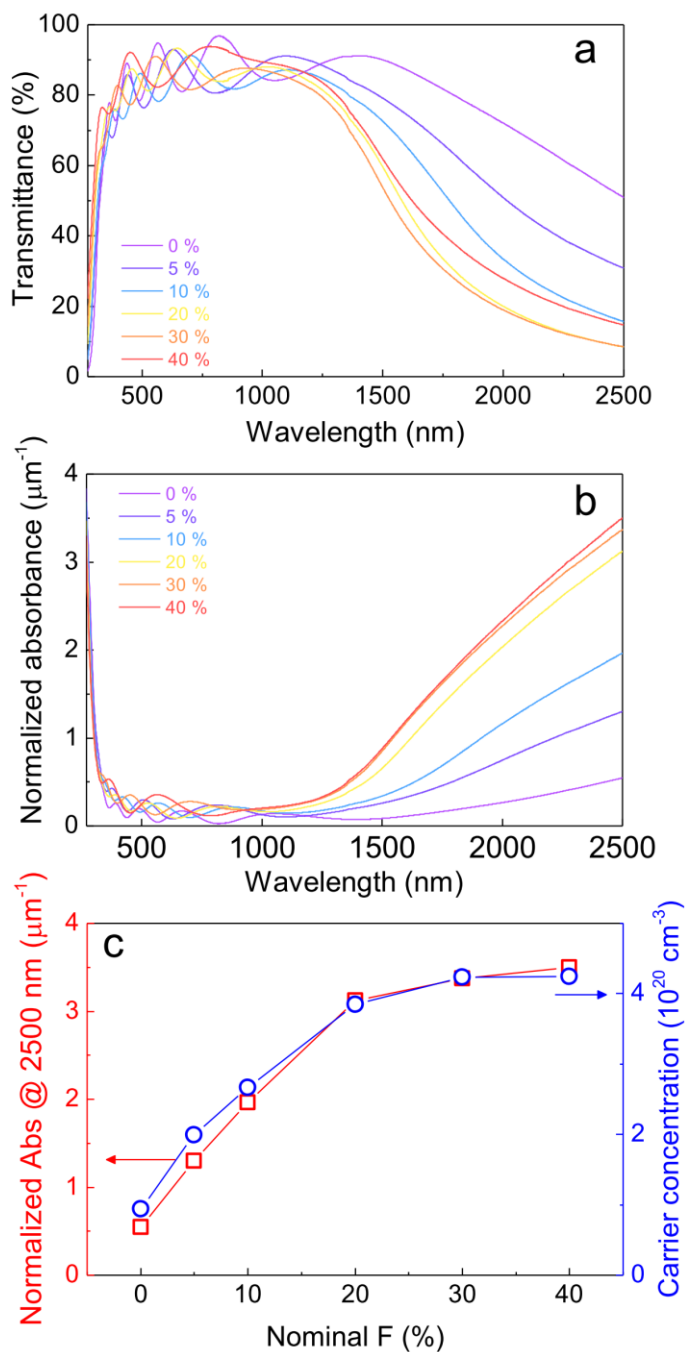


Figure S9. Tauc plots for FTO thin films deposited at 440 °C as a function of fluorine concentration.

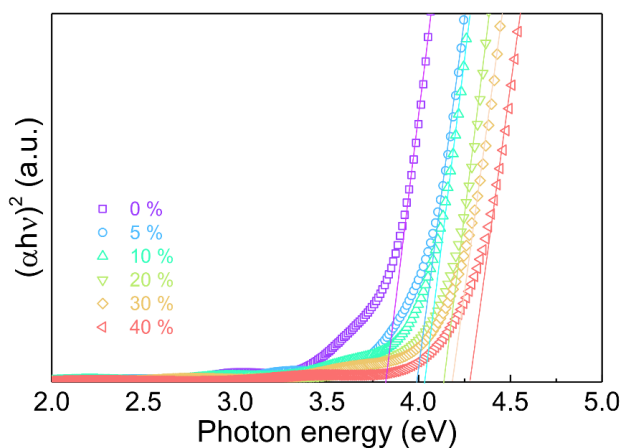


Figure S10. XPS spectra of F1s, Sn4d and valence band regions for SnO₂ and FTO20 deposited at 440 °C.

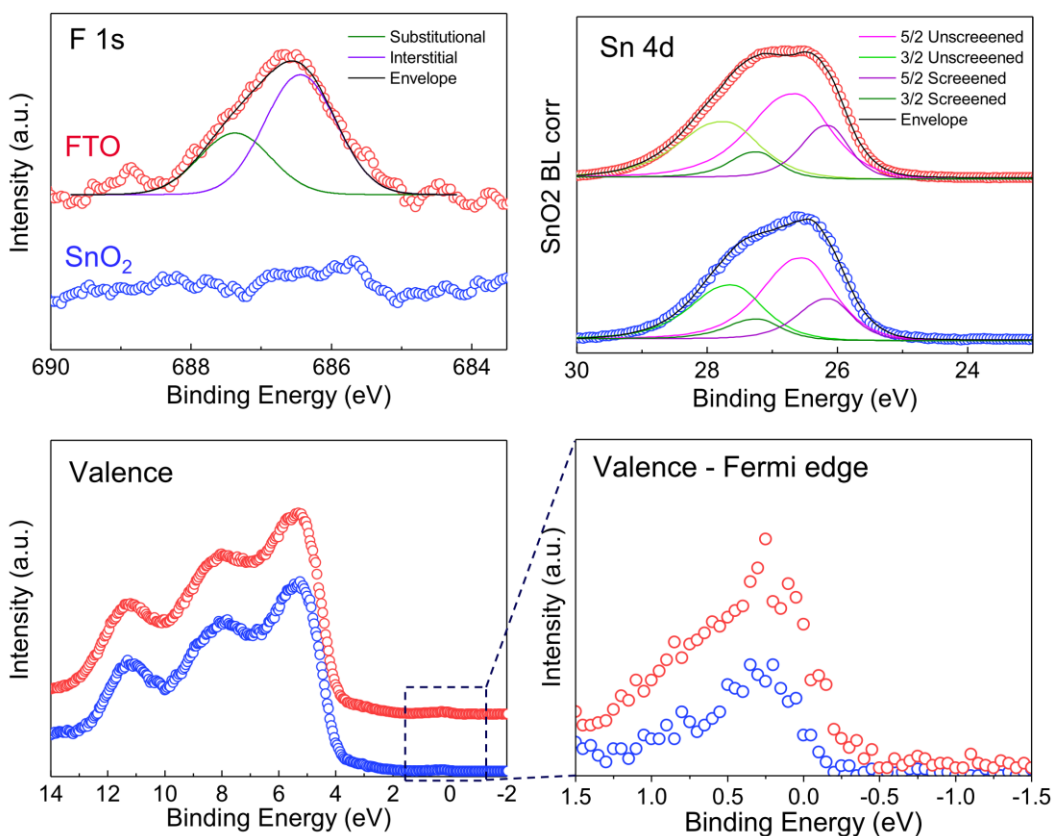


Figure S11. Maximum penetration depth using a Berkovich tip under a constant applied load of 1100 μN for FTO samples deposited at various temperatures.

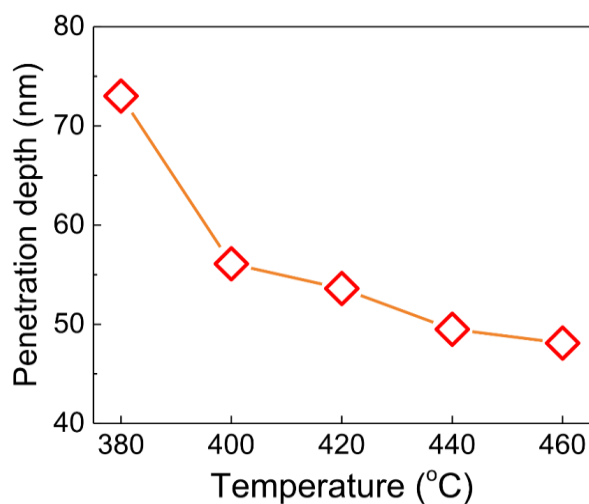


Figure S12. Elastic modulus and hardness for FTO thin films deposited at 440 °C as function of fluorine concentration.

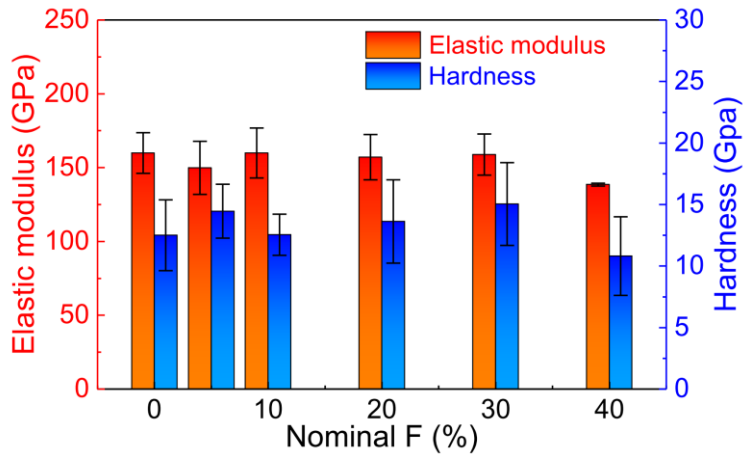
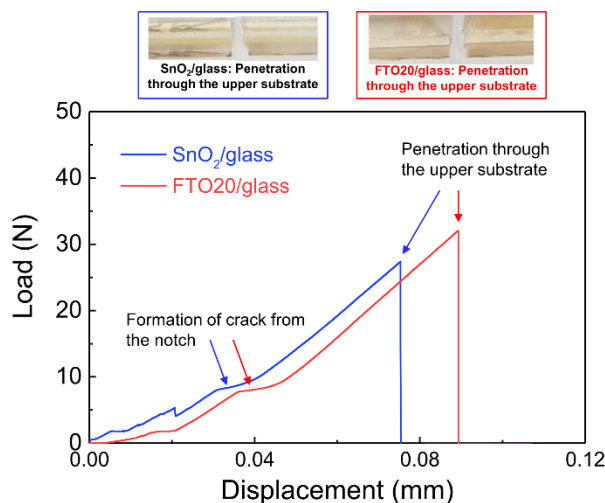


Figure S13. Typical load-displacement behavior obtained from 4-point bending test for SnO₂/glass (blue) and FTO20/glass (red). The pictures of the fractured samples after concluding the test are also shown.



The 4-point bending test can quantitatively measure the interfacial toughness (or interfacial adhesion energy) of a thin film deposited on a substrate, provided that the interface is not strong enough to prevent delamination. First, the SnO₂ and FTO samples (30×30 mm²) were bonded with bare borosilicate glass using a EPO-TEK 353ND glue, to create a sandwich structure where the thin coating is in the middle. The samples were then diced into rectangular pieces of 30 × 3mm² and cured at 120 °C for 2 h. A notch was made on the back of the substrate with a diamond blade, penetrating roughly 80% into the substrate thickness and getting in proximity of the interface between glass and SnO₂/FTO. This process is necessary to induce crack formation. Then the samples are subject to 4-point bending test with the aim of propagating the crack, and from the load-displacement curves the energy release due to crack propagation can be measured. The detailed description of 4-point bending experimental method and equations are presented elsewhere ^{1, 2}.

When the crack propagated to the interface of interest, two scenarios can happen: the crack deviates and propagates across the interface causing debonding and delamination, or the crack propagates through the interface. In the first case, we have a weak interface and the interfacial energy can be actually measured. In the second case, the bonding between film and substrate is very strong and the interfacial energy cannot be measured, but conclusions can be drawn regarding its high value. In our experimental results, the interfacial bonding between SnO₂/FTO and the glass substrate is strong, and in all the performed tests (at least 5 separate tests per sample composition) the crack penetrated through upper substrate without

any delamination. This is not surprising if we consider the potential chemical interaction between tin and silicon dioxide with formation of Sn-O-Si bond during the pyrolysis process³.

Table S1. Electrical and optical properties for some of the FTO films presented in this study.

| Deposition temp. (°C) | Doping (%) | Carrier conc. (10^{20}cm^{-3}) | Mobility (cm^2/Vs) | Resistivity ($\times 10^{-4} \Omega\text{cm}$) | Average visible Transmittance (%) | Peak visible Transmittance (%) | Band gap (eV) |
|-----------------------|------------|-------------------------------------------|--------------------------------------|--------------------------------------------------|-----------------------------------|--------------------------------|---------------|
| 380 | | 1.1 | 6.6 | 170.1 | 77.1 | 86.9 | 3.43 |
| 400 | | 3.3 | 10.8 | 17.7 | 82.0 | 90.7 | 4.00 |
| 420 | 20 | 4.6 | 18.7 | 7.3 | 85.5 | 93.7 | 4.08 |
| 440 | | 3.9 | 22.2 | 7.3 | 86.3 | 93.3 | 4.11 |
| 460 | | 2.5 | 27.0 | 9.3 | 76.9 | 87.9 | 3.67 |
| | 0 | 0.9 | 14.5 | 45.5 | 84.7 | 94.8 | 3.77 |
| | 5 | 2.0 | 24.3 | 12.9 | 83.4 | 93.0 | 3.94 |
| 440 | 10 | 2.7 | 22.6 | 10.4 | 83.4 | 91.3 | 3.99 |
| | 20 | 3.9 | 22.2 | 7.3 | 86.3 | 93.3 | 4.11 |
| | 30 | 4.2 | 20.1 | 7.3 | 84.0 | 91.1 | 4.14 |
| | 40 | 4.2 | 19.3 | 7.6 | 88.3 | 93.1 | 4.24 |

Supporting References

1. Kim, J.-W.; Jeong, M.-H.; Park, Y.-B., Effect of HF & H₂SO₄ pretreatment on interfacial adhesion energy of Cu–Cu direct bonds. *Microelectronic Engineering* **2012**, *89*, 42-45.
2. Kim, J.-W.; Kim, K.-S.; Lee, H.-J.; Kim, H.-Y.; Park, Y.-B.; Hyun, S.-M., Characterization and observation of Cu-Cu Thermo-Compression Bonding using 4-point bending test system. *Journal of the Microelectronics and Packaging Society* **2011**, *18* (4), 11-18.
3. Kobets, A. V.; Vorobyova, T. N.; Vrublevskaya, O. N.; Reva, O. V.; Kuznetsov, B. V., Multilayer Metal Film Plating on Glass. *Journal of Adhesion Science and Technology* **2012**, *25* (11), 1277-1287.